Comparison of automatic and interactive thresholding of hemispherical photography

A. Inoue[1], K. Yamamoto[2], N. Mizoue[3]

[1]*Laboratory of Forest Ecology, Faculty of Environmental and Symbiotic Sciences, Prefectural University of Kumamoto, Kumamoto, Japan*
[2]*Laboratory of Forest Environment and Resources, Graduate School of Bioagricultural Sciences, Nagoya University, Nagoya, Japan*
[3]*Laboratory of Forest Planning, Faculty of Agriculture, Kyushu University, Fukuoka, Japan*

ABSTRACT: This study presents the effects of operator bias and variation in interactive thresholding on the estimation of light environment using hemispherical photography. Twenty-one hemispherical photographs taken beneath a wide range of canopy densities were visually converted to binary images twice by 21 operators, and then the gap fraction was computed from the images. The interactive threshold varied greatly among the different operators and within a single operator, which resulted in a considerable operator bias and variation in the gap fraction. This study also compared three widely used automatic thresholding algorithms, which were installed in freely available software LIA for Win32 for analyzing hemispherical photography, with interactive thresholding using the same photographs. The median of the interactive threshold by repetitive interactive thresholdings from 21 operators was assumed to be correct for the comparison. The results indicated that MINIMUM was considered to be a better algorithm than the other ones installed in LIA32 when the gap fraction was over 10%. However, VARIANCE seemed to be superior to MINIMUM under the low gap fraction and the cloudy sky condition with dark and white clouds. This implied that MINIMUM or VARIANCE should be used for analyzing hemispherical photographs with LIA32. In conclusion, we need to pay attention to the selection of the automatic thresholding algorithm and the sky condition when taking hemispherical photographs.

Keywords: image analysis; LIA for Win32; light environment; operator bias; operator variation

Hemispherical photography has made it possible to estimate the potential direct and diffuse light that penetrates through discrete canopy openings, and also to provide a permanent record of the position, size, density and distribution of canopy openings (Rich 1990; Jonckheere et al. 2004). Studies have been facilitated by the recent availability of inexpensive digital cameras that can be equipped with fish-eye lenses. Digital hemispherical photography is potentially useful in spatially and temporally intensive studies, since it eliminates the cost, time and labour associated with film processing and image scanning (Englund et al. 2000; Frazer et al. 2001; Hale, Edwards 2002; Inoue et al. 2002, 2004a,b; Ishida 2004; Jonckheere et al. 2004; 2005). The technique has the added advantage that the images can be viewed immediately in the field and retaken if necessary (Frazer et al. 2001; Hale, Edwards 2002; Jonckheere et al. 2004). These features have contributed to making hemispherical photography one of the most effective devices in estimating the forest light environment.

One of the most important problems on hemispherical photography is the difficulty associated with distinguishing the foliage, branches and stems of trees from the background sky (Barrie et al. 1990; Rich 1990; Roxburgh, Kelly 1995; Machado, Reich 1999; Englund et al. 2000; Kato, Komiyama 2000; Frazer et al. 2001; Jonckheere et al. 2004, 2005; Nobis, Hunziker 2005; Cescatti 2007; Jarcuska et al. 2010). Most studies classify images into sky and canopy using an operator-defined threshold obtained by visually comparing the classified image with the original image (e.g. Barrie et al. 1990; Roxburgh, Kelly 1995; Inoue et al. 1996; Machado, Reich 1999; Englund et al. 2000; Hale 2001, 2003; Hale, Edwards 2002). This operator-dependent step is called "interactive thresholding" and is the only subjective stage of the estimation process (Barrie et al. 1990; Frazer et al. 2001). This subjectivity means that interactive thresholding is likely to be subject to operator bias and variation: the differences in the estimation among different operators and within a single operator, respectively (Rich et al. 1993; Easter, Spies 1994; Weaver, Au 1997; Englund et al. 2000; Kato, Komiyama 2000; Ishida 2004; Jonckheere et al. 2004, 2005; Nobis, Hunziker 2005; Cescatti 2007). As Machado and Reich (1999) pointed out, small changes in the threshold could have a large effect on the light environment estimate, and hence the interactive thresholding may produce operator bias and variation in the estimation of the light environments. Nobis and Hunziker (2005) compared the interactive thresholds determined three times by seven operators with their averages using 20 photographs, and reported that the interactive thresholds varied greatly. However, they did not distinguish operator bias and variation. Jonckheere et al. (2005) also examined the operator bias in the gap fraction among 10 operators using 10 photographs, and found that the operator bias increased as the gap fraction increased. The operator bias was, however, studied beneath comparatively open canopies, i.e. the gap fraction > 30% (Jonckheere et al. 2005). Hemispherical photography is often used to estimate the light environment beneath dense canopies (e.g. Barrie et al. 1990; Roxburgh, Kelly 1995; Inoue et al. 1996, 2002; Machado, Reich 1999; Englund et al. 2000; Kato, Komiyama 2000; Hale 2001, 2003; Hale, Edwards 2002; Nobis, Hunziker 2005). It is therefore necessary to investigate the operator bias and variation in interactive thresholding and their effects on the estimation of light environments across a wide range of canopy densities.

Interactive thresholding is also too time- and labour-consuming to apply to large numbers of photographs (Weaver, Au 1997; Nobis, Hunziker 2005). By contrast, an automatic thresholding algorithm enables us to convert hemispherical photographs to binary images not subjectively but objectively, and to reduce greatly the time and labour required for the thresholding. For this reason various automatic thresholding algorithms have been developed and compared (Kato, Komiyama 2000; Ishida 2004; Jonckheere et al. 2005; Nobis, Hunziker 2005; Cescatti 2007). Kato and Komiyama (2000) devised a method for determining the threshold of hemispherical photographs taken in a deciduous broadleaved forest. In this method, the threshold is determined based on the relationship between the measured indirect site factor (ISF) using the quantum sensors and the estimated ISF from the photographs. However, as Ishida (2004) pointed out, the method cannot be directly applied to other types of forests, since the relationship would vary with the forest type. Ishida (2004) proposed an automatic algorithm for determining the threshold with the maximum curvature on a histogram from hemispherical photography, but the algorithm has not been compared with other automatic algorithms and interactive thresholding. Nobis and Hunziker (2005) developed an automatic algorithm, SideLook, for determining a threshold based on the edge detection, and compared the algorithm with interactive thresholding. Although Nobis and Hunziker (2005) found that the gap fractions from SideLook and the interactive thresholding were highly correlated, SideLook has not been compared with the other automatic thresholding algorithms. Jonckheere et al. (2005) compared 35 automatic thresholding algorithms and interactive thresholding, and suggested that the iterative automatic algorithm proposed by Ridler and Calvard (1978) was the most reliable method. Cescatti (2007) devised an automatic thresholding method based on the linear conversion of hemispherical photographs, LinearRatio, and compared this method with the plant canopy analyzer, interactive thresholding, iterative thresholding (Ridler, Calvard 1978) and SideLook (Nobis, Hunziker 2005). The results showed that LinearRatio produced a good estimation of the canopy transmittance, whereas the iterative thresholding led most likely to overestimation (Cescatti 2007). Jarcuska et al. (2010) also compared the light environment estimates from two programmes for the analysis of hemispherical photograph, i.e. Gap Light Analyzer (e.g. Frazer et al. 2001) and WinScanopy (e.g. Petritan et al. 2009), with different automatic thresholding algorithms. Despite of these efforts, it cannot be concluded which automatic thresholding algorithm is the most reliable.

Recently, various computerized programmes for analyzing hemispherical photography have been developed (e.g. Steege 1993; Frazer et al. 2001; Ishida 2004; Petritan et al. 2009). Among these programmes, LIA for Win32 (LIA32: Copyright K. Yamamoto) is one of the most useful image-processing programmes, which is developed by Delphi 5.0J (Inspire Corporation, Scot Valley, USA) and available freely at http://www.agr.nagoya-u.ac.jp/~shinkan/LIA32/index-e.html. LIA32 includes three widely used automatic thresholding algorithms proposed by Otsu (1979), Kapur et al. (1985) and Kittler and Illingworth (1986). However, it is unclear which algorithm is the most reliable when classifying a hemispherical photograph into the sky and canopy automatically. To establish a procedure for analyzing hemispherical photography using LIA32, there is a need for comparison of these algorithms and evaluation of their reliabilities.

The objectives of this study were

(1) to examine the effects of operator bias and variation in interactive thresholding on the estimation of light environment using digital hemispherical photography;

(2) to examine which automatic thresholding algorithm included in LIA32 can be effectively applied to digital hemispherical photography by comparing the results from interactive thresholding.

MATERIALS AND METHODS

Study area

The study was conducted in the Hiruzen Experimental Forest of Tottori University in Okayama Prefecture, western Japan (35°18'N and 133°35'E). The average annual temperature, average annual precipitation and maximum snow fall in the Experimental Forest were 11.3°C, 2,140 mm and 2.1 m, respectively (Wang and Uozumi 2001). The soils are mainly grey volcanic ash soils. A circular plot of 0.02 ha was established in three stands for each forest type: *Cryptomeria japonica* (CJ1-3), *Chamaecyparis obtusa* (CO1-3), *Pinus densiflora* (PD1-3), *Larix kaempferi* (LK1-3) and deciduous broadleaved species (BL1-3). CJ, CO, PD and LK were even-aged pure stands, whereas BL were uneven-aged mixed stands. BL were dominated by *Quercus serrata*, *Quercus acutissima* and *Castanea crenata*. On each plot, total tree height and diameter at 1.2 m (dbh) of all living trees were measured. A general description of each plot is shown in Table 1.

Hemispherical photography

At a sample point selected randomly on each plot, a colour hemispherical photograph was taken under still and cloudy conditions (Rich 1990)

Table 1. General description of each plot

Plot	Species	Tree height (m)*	dbh (cm)*	Stand density (stems·ha^{-1})
CJ1	*Cryptomeria japonica*	22.6 ± 2.1	41.6 ± 6.5	450
CJ2	*Cryptomeria japonica*	21.1 ± 2.9	32.9 ± 7.5	850
CJ3	*Cryptomeria japonica*	10.9 ± 1.6	15.7 ± 3.6	2700
CO1	*Chamaecyparis obtusa*	16.8 ± 0.8	27.0 ± 4.0	750
CO2	*Chamaecyparis obtusa*	10.6 ± 0.6	16.7 ± 2.2	1,300
CO3	*Chamaecyparis obtusa*	14.1 ± 1.0	18.0 ± 3.2	1,550
PD1	*Pinus densiflora*	21.2 ± 1.0	43.0 ± 4.6	1,550
PD2	*Pinus densiflora*	22.2 ± 1.8	33.0 ± 6.9	500
PD3	*Pinus densiflora*	12.5 ± 1.7	20.0 ± 3.9	1,100
LK1	*Larix kaempferi*	17.6 ± 1.3	21.9 ± 3.4	1,050
LK2	*Larix kaempferi*	15.0 ± 4.0	18.3 ± 6.5	1,050
LK3	*Larix kaempferi*	13.0 ± 5.4	15.1 ± 8.0	1,050
BL1	Broad-leaved species**	12.9 ± 1.8	18.6 ± 5.4	500
BL2	Broad-leaved species**	12.8 ± 7.8	15.1 ± 10.3	900
BL3	Broad-leaved species**	12.3 ± 2.0	23.5 ± 8.0	1,150

*Average ± Standard Deviation, **The dominant broad-leaved species in BL were *Quercus serrata*, *Quercus acutissima* and *Castanea crenata* using a digital camera (Coolpix 990, Nikon Corporation, Tokyo, Japan) with a fish-eye lens (Fish-eye converter FC-E8, Nikon Corporation, Tokyo, Japan). The camera was mounted at a height of 1.2 m above the ground on a tripod and levelled with a bubble level. An automatic setting for aperture width and shutter speed was used (Englund et al. 2000; Inoue et al. 2002, 2004a,b; Jarcuska et al. 2010). Inoue et al. (2004b) found no effects of different image quality and size of the Coolpix 990 on light environment estimates, and therefore the fine-quality and XGA-size image (1,024 pixel × 768 pixel) was used in this study. Photographs of LK and BL were taken twice (before and after leaf flushing) to cover a wide range of canopy densities, which increased the total number of photographs used in this study to 21.

Interactive thresholding

The hemispherical photographs were downloaded directly from the digital camera to a personal computer with a CRT display (FM-V Deskpower M2/457, Fujitsu Corporation, Tokyo, Japan). To examine the operator bias, all 21 hemispherical photographs were visually converted to binary (black-and-white) images by 21 operators: one operator was well-experienced, whereas others had no experiences with interactive thresholding and with the evaluation of hemispherical photography. Since the blue channel image enables us to obtain a maximum contrast between the tree crown and the background sky among blue, red and green-filtered grey level images (Lee et al. 1983; Nobis, Hunziker 2005), colour and blue channel images were simultaneously displayed on a computer display. Using the Photoshop Elements 2.0 image-processing software (Adobe Systems Incorporated, San Jose, USA), each operator determined a threshold for each of the grey-scale images by interactively changing the threshold up or down and visually comparing the resulting black-and-white image with the colour image, until the edge between the tree crown and the background sky in the classified image best matched that observed in the colour image. To assess the operator variation, the interactive thresholding procedure was repeated twice by all operators with a one-week interval using a different order of photographs. For interactive thresholding, the contrast and brightness of the CRT display were maintained constant regardless of the operator. The interactive threshold is referred to as IT.

Automatic thresholding

The widely used automatic thresholding algorithms proposed by Otsu (1979), Kapur et al. (1985) and Kittler and Illingworth (1986) were thus applied to the blue channel images. In these algorithms, the optimal thresholds are based on between-class variance, classification error and total entropy, respectively, described briefly as follows: in this study these three algorithms are referred to as VARIANCE, MINIMUM and ENTROPY, respectively.

An image can be described as being composed of L grey levels. The number of pixels at a grey level i is denoted by n_i, and the total number of pixels is given by $N = n_1 + n_2 + \ldots + n_L$. The probability of a pixel having a given grey level is thus:

$$p_i = n_i/N$$

where: $p_i \geq 0$, $\sum_{i=1}^{L} p_i = 1$

Now suppose that we are classifying the pixels into two classes: those with grey levels up to threshold k, $(1, \ldots, k)$ and those with grey levels above threshold k $(k + 1, \ldots, L)$. The probabilities of class occurrence, class mean levels, class variances and class entropies, are given by

$$\omega_0 = \sum_{i=1}^{k} p_i, \quad \omega_1 = \sum_{i=k+1}^{L} p_i$$

$$\mu_0 = \sum_{i=1}^{k} i p_i / \omega_0, \quad \mu_1 = \sum_{i=k+1}^{L} i p_i / \omega_1$$

$$\sigma_0^2 = \sum_{i=1}^{k} (i-\mu_0)^2 p_i / \omega_0, \quad \sigma_1^2 = \sum_{i=k+1}^{L} (i-\mu_1)^2 p_i / \omega_1$$

and

$$E_0 = -\sum_{i=1}^{k} \frac{p_i}{\omega_0} \log \frac{p_i}{\omega_0}, \quad E_1 = -\sum_{i=k+1}^{L} \frac{p_i}{\omega_1} \log \frac{p_i}{\omega_1}, \text{ respectively.}$$

Then, the between-class variance $\sigma_B^2(k)$, classification error $J(k)$ and total entropy $\Psi(k)$ are defined as:

$$\sigma_B^2(k) = \omega_0 \omega_1 (\mu_0 - \mu_1)^2$$

$$J(k) = \omega_0 \log\left(\frac{\sigma_0}{\omega_0}\right) + \omega_1 \log\left(\frac{\sigma_1}{\omega_1}\right)$$

and $\psi(k) = E_0 + E_1$, respectively.

These measures are calculated for $i = 0, \ldots, L-1$, and the optimal thresholds ATv (for VARIANCE), ATm (for MINIMUM) and ATe (for ENTROPY) are determined for the values of k at which $\sigma_B^2(k)$ and $\Psi(k)$ are maximized and $J(k)$ is minimized, respectively. These automatic thresholding algorithms were performed using the LIA32.

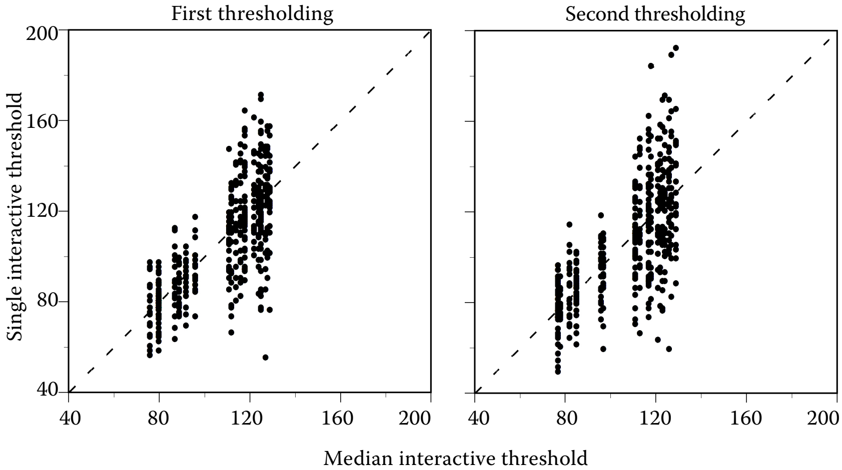

Fig. 1. Scatter plots of the single interactive threshold in relation to the robust mean interactive threshold values. The broken lines indicate 1:1

Evaluation of light environment

All hemispherical photographs were converted to binary images according to each of the interactive and automatic thresholds, i.e. IT, ATv, ATm and ATe. The gap fraction was then computed from the binary images as a measure of the light environment. The gap fraction was defined as the total amount of sky visible as a proportion of the entire hemisphere when viewed from a point (Inoue et al. 2004b). The fish-eye lens used in this study was designed to produce a simple polar projection (Herbert 1987), but it did not conform exactly to this design specification (Englund et al. 2000; Frazer et al. 2001; Inoue et al. 2004a). The gap fraction was therefore computed by calibrating the view angle and lens distortion of the fish-eye converter using the LIA32 (Inoue et al. 2004a).

Statistical analyses

To assess the operator bias in interactive thresholding, the ranges in IT and gap fraction among the 21 operators were calculated for each photograph. For this analysis, to distinguish the operator bias and variation clearly, the ranges obtained from the thresholdings performed in duplicate were treated individually. To evaluate the operator variation in the interactive thresholding, IT and gap fraction were compared between the first and the second thresholding for each operator using Wilcoxon's rank sign test. Since there was no correct answer in determining the threshold for each hemispherical photograph, the median of IT by the two interactive thresholdings from 21 operators was assumed to be correct and used for the comparison of automatic thresholding algorithms with the interactive thresholding. The threshold and gap fraction were compared between the automatic thresholding algorithms and interactive thresholding using Spearman's correlation coefficient by rank test and Wilcoxon's rank sign test. For these statistical analyses, all percentage data of gap fraction was transformed by arcsin. Statistical analyses were performed using Excel 2000 with the add-in software Statcel 2 (Yanai 2004).

RESULTS

Operator bias

Fig. 1 shows the scatter plots of the single interactive threshold (IT) in relation to the median

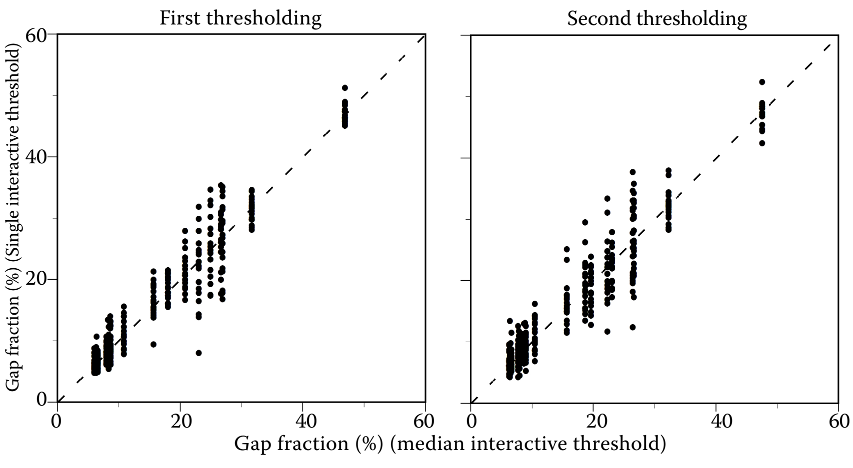

Fig. 2. Scatter plots of the gap fraction from the single interactive threshold in relation to that from the robust mean interactive threshold values. The broken lines indicate 1:1

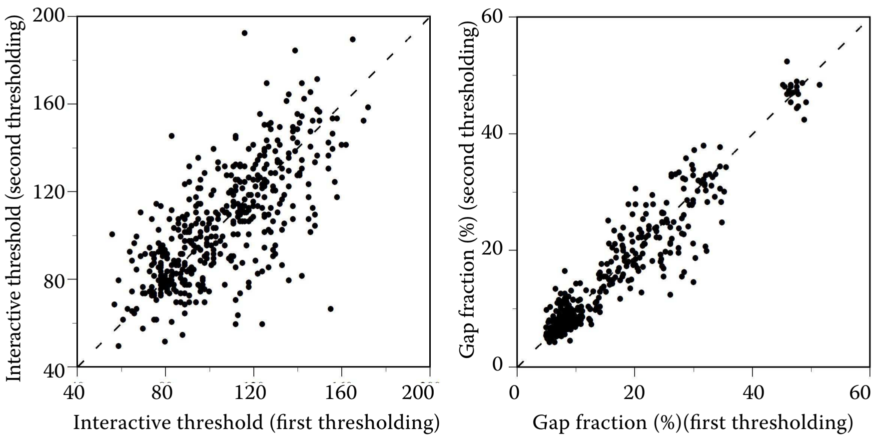

Fig. 3. Comparisons of interactive threshold and gap fraction between first and second thresholdings. The broken lines indicate 1:1

interactive threshold values. For both the first and the second interactive thresholdings, IT for each photograph varied greatly according to operators. The respective average and maximum ranges of IT were 58 and 94 for the first thresholding and 71 and 110 for the second thresholding. Such an operator bias in IT produced a remarkable operator bias in gap fraction (Fig. 2). The respective average and maximum ranges of the gap fraction were 8.7% and 23.9% for the first thresholding and 10.3% and 25.2% for the second thresholding.

Operator variation

Fig. 3 compares IT and gap fraction between the first and the second thresholdings. For 11 out of the 21 operators, IT differed significantly between the two thresholdings ($P < 0.05$). For all operators, the average and maximum difference in IT between the two thresholdings was 0 and 88, respectively. Gap fraction estimates from the same 11 operators were significantly different between the two thresholdings ($P < 0.05$). For the 21 operators, the average and maximum difference in gap fraction between the repetitive thresholdings was 0.2% and 15.3%, respectively.

Comparison of interactive thresholding with automatic thresholding algorithms

Fig. 4 compares the threshold and gap fraction between the median interactive thresholding and three automatic thresholding algorithms. Although there was a significant correlation between ATv and IT ($r = 0.716$; $P < 0.01$), ATv was significantly smaller than IT ($P < 0.001$). There was no significant difference between ATm and IT ($P = 0.170$), and no significant correlation between ATm and IT was found out ($r = –0.378$; $P = 0.090$). ATe was excessively smaller than IT ($P < 0.001$), whereas ATe was significantly correlated with IT ($r = 0.700$; $P < 0.01$).

The gap fraction from ATv was significantly correlated with that from IT ($r = 0.940$; $P < 0.001$) and was significantly higher than that from IT ($P < 0.001$), with the average and maximum difference in gap fraction being 4.3% and 14.5%, respectively. There were no significant differences in gap fraction between ATm and IT ($P = 0.394$), and the gap fraction from ATm was not correlated with that from IT ($r = 0.404$; $P = 0.071$). However, when three outliers, of which gap fractions from ATm were less than 3%, were excluded from statistical analyses, the gap fraction from ATm was

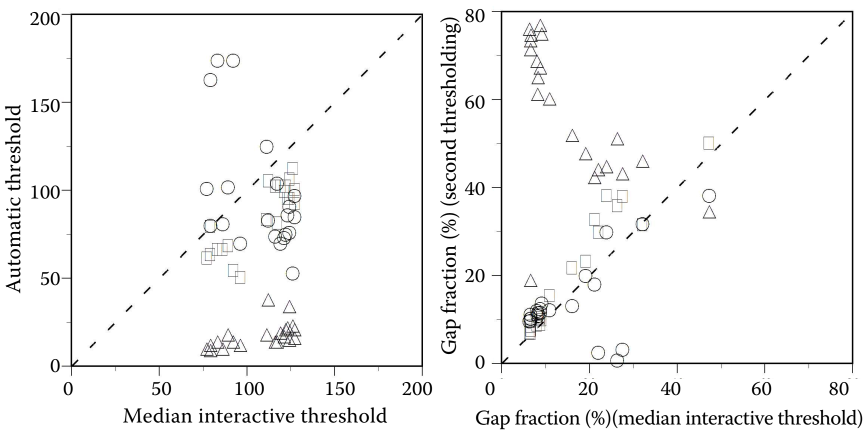

Fig. 4 Comparisons of threshold and gap fraction between the interactive thresholding and three automatic thresholding algorithms. The broken lines, squares, circles and triangles indicate 1:1, VARIANCE, MINIMUM and ENTROPY, respectively

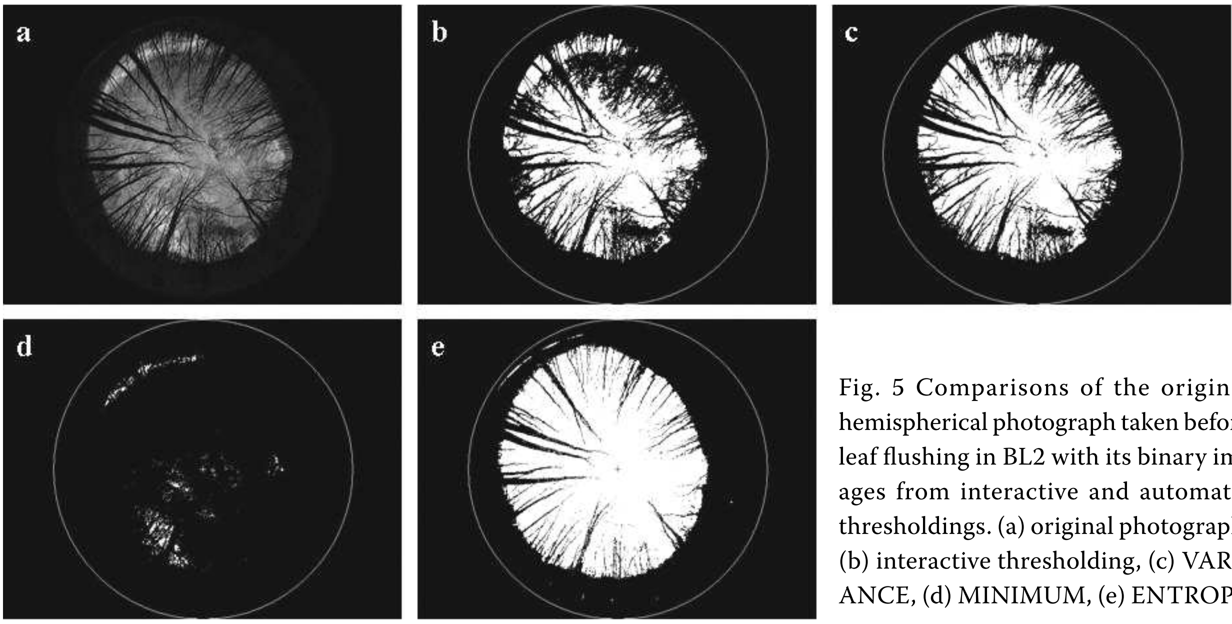

Fig. 5 Comparisons of the original hemispherical photograph taken before leaf flushing in BL2 with its binary images from interactive and automatic thresholdings. (a) original photograph, (b) interactive thresholding, (c) VARIANCE, (d) MINIMUM, (e) ENTROPY

strongly correlated with that from IT (r = 0.953; P < 0.001), whereas there was a significant difference in gap fractions between ATm and IT (P < 0.05). These three photographs that produced the outliers were taken before leaf flushing on the plots of BL2, LL1 and LL3. For example, the original photograph taken in BL2 and its binary images from the interactive and automatic thresholdings are given in Fig. 5. There was a negative correlation between the gap fraction from ATe and IT (r = –0.649, P < 0.01), and the gap fraction from ATe was significantly higher than that from IT (P < 0.001). The average and maximum difference in gap fraction between ATe and IT was 41.3% and 69.9%, respectively.

DISCUSSION

Operator bias and variation

The gap fraction for each plot in this study, calculated as the median of two interactive thresholdings by 21 operators, ranged from 5.3% to 47.1%, indicating that our data covered a wider range of gap fraction than the previous study (Jonckheere et al. 2005).

As shown in Figs. 1 and 2, the single interactive threshold varied greatly among the different operators, resulting in a remarkable operator bias in gap fraction. This finding was in accordance with those reported by Jonckheere et al. (2005) and Nobis and Hunziker (2005). Jonckheere et al. (2005) examined the operator bias in gap fraction among 10 operators using 10 photographs taken beneath comparatively open canopies, i.e. the gap fraction was over 30%, and reported that the bias became larger as the gap fraction of the photograph increased. Similarly, our data showed that the operator bias, when the gap fraction was less than 30%, became larger as the gap fraction increased. However, the operator bias was steady at a constant level when the gap fraction was over 30%. The reason for the inconsistency between these studies is not clear, but it may be due to the differences in operators and/or in light conditions, indicating that the interactive thresholding makes it impossible to compare the results from different studies.

For more than a half of the operators serving in this study, IT and gap fraction were significantly different between the repetitive thresholdings (see Fig. 3). To reduce the operator variation, images are generally analyzed several times by a single operator, and then an average of the analyses is taken for all outputs (e.g. Machado, Reich 1999; Englund et al. 2000; Frazer et al. 2001; Hale, Edwards 2002; Hale 2003; Nobis, Hunziker 2005). Such a procedure would be effective in reducing the operator variation in the interactive thresholding, but it does not work for eliminating the operator bias. To obtain a reliable threshold by the interactive thresholding, it would be necessary for the photographs to be analyzed several times not by a single operator but by several different operators. However, repetitive thresholding by several operators will be impractical in spatially and temporally intensive studies, since the interactive thresholding is too time- and labour-consuming.

These results suggest that the reproducibility of interactive thresholding is questionable, and it is difficult to yield consistent estimations of light environment using interactive thresholding within a single operator as well as between operators. Therefore, both operator bias and variation in interactive thresholding must be considered in the estimation of light environments using hemispherical photography. There is a need for alternatives to interactive thresholding, so that different studies can be compared based on objective criteria.

Comparison of interactive thresholding with automatic thresholding algorithms

Fig. 4 clearly showed that ENTROPY proposed by Kapur et al. (1985) overestimated the gap fraction compared to interactive thresholding. As shown in Fig. 5a and e, the grey levels of small branches (and foliage in other photographs) were most likely mistaken for those of the background sky, resulting in the overestimation of gap fraction. This result indicates that ENTROPY is an unprofitable automatic algorithm for converting colour hemispherical photographs to binary images. For the high gap fraction (> 10%), the gap fractions from MINIMUM proposed by Kittler and Illingworth (1986) and interactive thresholding corresponded well, except for the three outliers as mentioned above. However, for the low gap fraction (< 10%), VARIANCE proposed by Otsu (1979) showed a slightly smaller difference in the gap fraction from interactive thresholding than MINIMUM. Therefore it could not be concluded which algorithm, VARIANCE or MINIMUM, is superior to the other from the results of this study.

Jonckheere et al. (2005) compared the performance of 35 automatic thresholding algorithms based on the average thresholding performance score (AVE) proposed by Sezgin and Sankur (2004) and concluded that the iterative algorithm devised by Ridler and Calvard (1978) was the most reliable automatic thresholding algorithm. Nevertheless, Cescatti (2007) showed that Ridler and Calvard's iterative thresholding algorithm (Ridler and Calvard 1978) produced the greatest overestimation of canopy transmittance compared to interactive thresholding, SideLook (Nobis and Hunziker 2005) and LinearRatio (Cescatti 2007). According to the AVE scores of Jonckheere et al. (2005), VARIANCE and MINIMUM were evaluated as the best and the worst algorithm, respectively, among the three algorithms applied in this study. The result of this study, however, showed that MINIMUM was a better algorithm compared to VARIANCE when the gap fraction was over 10%. These findings suggest that the optimal automatic thresholding algorithm may vary with the light conditions of the stand. Although there is no statement with regard to the range of gap fractions of the photographs used in the study (Jonckheere et al. 2005), this inconsistency suggests that the iterative algorithm (Ridler and Calvard 1978) may not work well for converting the hemispherical photographs to binary images, depending on the light conditions of the stand. Hemispherical photography is used to estimate a wide range of light environments beneath various canopy densities of stands, and thus we should pay attention to the selection of the automatic thresholding algorithm. Further comparison of the automatic thresholding algorithms is needed across a wide range of canopy densities by keeping a comparable character of the cloudy sky.

As shown in Fig. 4, excessively large differences in the gap fraction between MINIMUM and interactive thresholding were found for three photographs, whereas MINIMUM was considered to be a better algorithm than VARIANCE and ENTROPY for other photographs when the gap fraction was over 10%. These photographs were taken under conditions of cloudy sky with dark and white clouds (see Fig. 5a). It would be impossible to distinguish small branches from the background sky with MINIMUM, since there were parts of both dark and white in the background sky and the grey levels of dark clouds were mistaken for those of branches as shown in Fig. 5d. Even with interactive thresholding (Fig. 5b) and VARIANCE (Fig. 5c), the grey levels of dark clouds tended to be mistaken for those of small branches. These findings reveal that it is unfavourable to take hemispherical photographs when the sky is covered with clouds of different darkness, although the photographs should be taken under cloudy conditions to prevent halation (Rich 1990). It will therefore be necessary to take the hemispherical photography under uniform cloudy conditions or in the time before and after sunset.

CONCLUSIONS

In this study, the effects of operator bias and variation in interactive thresholding on the estimation of light environment using hemispherical photography were investigated across a wide range of canopy densities. This study also compared three widely used automatic thresholding algorithms with interactive thresholding. The results indicated that MINIMUM was considered to be a better algorithm than the other ones installed in LIA32 when the gap fraction was over 10%. However, VARIANCE seemed to be superior to MINIMUM under the low gap fraction and the conditions of cloudy sky with dark and white clouds. This implies that MINIMUM or VARIANCE should be used for analyzing hemispherical photographs with LIA32. This study also revealed that it is unfavourable to take hemispherical photographs when the sky is covered with clouds of different darkness. In conclusion, we need to pay attention to the selection of the automatic thresholding algorithm and the sky condition when taking hemispherical photographs, although the automatic algorithm enables us to greatly reduce time and labour for the thresholding of photographs and to yield consistent estimation of forest light environments. It is also necessary to install other automatic thresholding algorithms into LIA32 which will make LIA32 more useful software for analyzing hemispherical photography.

Acknowledgements

We would particularly like to thank Yuichiro Kawahara (graduate of Tottori University) for his assistance in the field. We also appreciate the English correction of Mr. Richard Steven Lavin, Faculty of Environmental and Symbiotic Sciences, Prefectural University of Kumamoto.

References

Barrie J., Greatorex-Davies J.N., Parsell R.J., Marrs R.H. (1990): A semi-automated method for analyzing hemispherical photographs for the assessment of woodland shade. Biological Conservation, ***54***: 327–334.

Cescatti A. (2007): Indirect estimates of canopy gap fraction based on the linear conversion of hemispherical photographs: Methodology and comparison with standard thresholding techniques. Agricultural and Forest Meteorology, ***143***: 1–12.

Easter M.J., Spies T.A. (1994): Using hemispherical photography for estimating photosynthetic photon flux density under canopies and in gaps in Douglas-fir forests of Pacific Northwest. Canadian Journal of Forest Research, ***24***: 2050–2058.

Englund S.R., O'brien J.J., Clark D.B. (2000): Evaluation of digital and film hemispherical photography and spherical densiometry for measuring forest light environments. Canadian Journal of Forest Research, ***30***: 1999–2005.

Frazer G.W., Fournier R.A., Trofymow J.A., Hall R.J. (2001): A comparison of digital and film fisheye photography for analysis of forest canopy structure and gap light transmission. Agricultural and Forest Meteorology, ***109***: 249–263.

Hale S.E. (2001): Light regime beneath Sitka spruce plantations in northern Britain: preliminary results. Forest Ecology and Management, ***151***: 61–66.

Hale S.E. (2003): The effect of thinning intensity on the below-canopy light environment in a Sitka spruce plantation. Forest Ecology and Management, ***179***: 341–349.

Hale S.E., Edwards C. (2002): Comparison of film and digital hemispherical photography across a wide range of canopy densities. Agricultural and Forest Meteorology, ***112***: 51–56.

Herbert T.J. (1987): Area projection of fish-eye photographic lenses. Agricultural and Forest Meteorology, ***39***: 215–223.

Inoue A., Okamura A., Mizoue N., Teraoka Y., Imada M. (1996): Estimation of relative illuminance in forests using hemispherical photographs. Journal of Forest Planning, ***2***: 125–129.

Inoue A., Yamamoto K., Mizoue N., Kawahara Y. (2002): Estimation of relative illuminance using digital hemispherical photography. Journal of Forest Planning, ***8***: 67–70.

Inoue A., Yamamoto K., Mizoue N., Kawahara Y. (2004a): Calibrating view angle and lens distortion of Nikon fish-eye converter FC-E8. Journal of Forest Research, ***9***: 177–181.

Inoue A., Yamamoto K., Mizoue N., Kawahara Y. (2004b): Effects of image quality, size, and camera type on forest light environment estimates using digital hemispherical photography. Agricultural and Forest Meteorology, ***126***: 87–96.

Ishida M. (2004): Automatic thresholding for digital hemispherical photography. Canadian Journal of Forest Research, ***34***: 2208–2216.

Jarcuska B., Kucbel S., Jaloviar P. (2010): Comparison of output results from two programmes for hemispherical image analysis: Gap Light Analyzer and WinScanopy. Journal of Forest Science, ***56***: 147–153.

Jonckheere I., Fleck S., Nackaerts K., Muys B., Coppin P., Weiss M., Baret F. (2004): Review of methods for in situ leaf area index determination. Part I. Theories, sensors and hemispherical photography. Agricultural and Forest Meteorology, ***121***: 19–35.

Jonckheere I., Nackaerts K., Muys B., Coppin P. (2005): Assessment of automatic gap fraction estimation of forests from digital hemispherical photography. Agricultural and Forest Meteorology, ***132***: 96–114.

Kapur J.N., Sahoo P.K., Wong A.K.C. (1985): A new method for grey-level picture thresholding using the entropy of the histogram. Computer Vision, Graphics, and Image Processing, ***29***: 273–285.

Kato S., Komiyama A. (2000): A calibration method for adjusting hemispherical photographs to appropriate black-and white images. Journal of Forest Research, ***5***: 109–111.

Kittler J., Illingworth J. (1986): Minimum likehood thresholding based on population mixture models. Pattern Recognition, ***25***: 1231–1240.

Lee Y.J., Alfaro R.I., Van Sickle G.A. (1983): Tree-crown defoliation measurement from digitized photographs. Canadian Journal of Forest Research, ***13***: 956–961.

Machado J., Reich P.B. (1999): Evaluation of several measures of canopy openness as predictors of photosynthetic photon flux density in deeply shaded conifer-dominated forest understory. Canadian Journal of Forest Research, ***29***: 1438–1444.

Nobis M., Hunziker U. (2005): Automatic thresholding for hemispherical canopy-photographs based on edge detection. Agricultural and Forest Meteorology, ***128***: 243–250.

Otsu N. (1979): A threshold selection method from grey-level histogram. IEEE Transactions on Systems, Man and Cybernetics, ***8***: 62–66.

Petritan A.M., von Lupke B., Petritan I.C. (2009): Influence of light availability on growth, leaf morphology and plant architecture of beech (*Fagus sylvatica* L.), maple (*Acer pseudoplatanus* L.) and ash (*Fraxinus excelsior* L.) sapling. European Journal of Forest Research, ***128***: 61–74.

Rich P.M. (1990): Characterizing plant canopies with hemispherical photographs. Remote Sensing Review, ***5***: 13–29.

Rich P.M., Clark D.B., Clark D.A., Oberbauer, S.F. (1993): Long-term study of solar radiation regimes in a tropical wet forest using quantum sensors and hemispherical photography. Agricultural and Forest Meteorology, ***65***: 107–127.

Ridler W., Calvard S. (1978): Picture thresholding using an iterative selection method. IEEE Transactions on Systems, Man and Cybernetics, ***8***: 260–263.

Roxburgh J.R., Kelly, D. (1995): Use and limitation of hemispherical photography for estimating forest light environments. New Zealand Journal of Ecology, ***19***: 213–217.

Sezgin M., Sankur B. (2004): Survey over image thresholding techniques and quantitative performance evaluation. Journal of Electronic Imaging, ***13***: 146–165.

Steege H.T. (1993): A Programme to Analyze Vegetation Indices Light and Quality from Hemispherical Photographs. Wegeningen, Tropenbos Documents 3: 44

Wang H., Uozumi Y. (2001): A study on the variation of relative stem-form and normal-factor in Japanese larch artificial forest. Journal of Japanese Forestry Society, ***83***: 197–203. (in Japanese with English summary)

Weaver J.L., Au J.L.S. (1997): Application of automatic thresholding in image analysis scoring of cells in human solid tumors labeled for proliferation markers. Cytometry, ***29***: 128–135.

Yanai H. (2004): Statcel -The Useful Add-in Software Forms on Excel- 2^{nd} Ed. Tokyo, OMS: 270. (in Japanese)

Received for publication July 5, 2010
Accepted after corrections November 22, 2010

Corresponding author:
Assoc. Prof. Akio Inoue, Laboratory of Forest Ecology, Faculty of Environmental and Symbiotic Sciences, Prefectural University of Kumamoto, Kumamoto 862-8502, Japan
e-mail: iakio@pu-kumamoto.ac.jp